

Phases of complex SYK from Euclidean wormholes

Hemant Rathi* and Dibakar Roychowdhury†

Department of Physics, Indian Institute of Technology Roorkee,
Roorkee 247667, Uttarakhand, India

Abstract

We present a JT gravity set up that reveals the evidence of (Euclidean) wormhole to black hole phase transitions at finite charge density and or chemical potential. We identify the low temperature *gapped* phase of the system as the charged wormhole solution that is conjectured to be dual to a two site complex SYK model at finite density. As the temperature of the system is increased, it passes over to a hot SYK phase which is dual to a two black hole system at finite density. Our analysis further reveals the existence of a (two site) Majorana SYK phase right at the critical point of the *first* order transition which glues the cold and the hot SYK phases together.

1 Introduction and summary

Wormholes are the geometrical bridges that connect the asymptotic regions of space-time [1]-[2]. These are the solutions of Einstein's equation in the classical limit.

Wormholes [3]-[10] are extensively studied in the context of JT gravity [11]-[13] that is conjectured to be dual to a SYK model [14]-[20]. In particular, the authors in [4] investigate a two site uncoupled Majorana SYK model that exhibits a *gapped* phase at low temperatures. The gravitational analogue of this phenomenon is proposed to be the Euclidean wormhole solution of JT gravity in the presence of matter couplings.

Authors in [6] further generalise their work considering a similar theory for Dirac fermions. In particular, they consider interactions by including the complex coupling between the two site Dirac SYK models and examine the corresponding thermodynamic properties using Schwinger-Dyson (*SD*) equation. Their model exhibits a first order phase transition in which a uncharged wormhole phase at low temperature disintegrates into a two black hole state at high temperatures¹.

The purpose of the present work is to carry out a parallel computation for the Dirac SYK model in the context of JT gravity and in particular, to explore the phase stability of the Euclidean wormhole solutions at finite charge density. In other words, our analysis to certain extent, complements those of the results of [6].

*E-mail: hrathi07@gmail.com, hrathi@ph.iitr.ac.in

†E-mail: dibakarphys@gmail.com, dibakar.roychowdhury@ph.iitr.ac.in

¹For higher dimensional wormholes and the associated phase structure see [21]-[24].

We propose the following modifications of the 2D Einstein-dilaton gravity in the presence of abelian one forms (A_μ)

$$S_{JT} \sim S_{EH} + \int d^2x \sqrt{-g} \left(a_1 \Phi^{2n} F^2 + a_2 \Phi^n \varepsilon^{\mu\nu} F_{\mu\nu} \right). \quad (1.1)$$

We further observe that the Chern-Simons (CS) term ($\sim \varepsilon^{\mu\nu} F_{\mu\nu}$) plays a pivotal role in constructing the wormhole solution. However, its contribution appears to be zero for the black hole phase. To summarise, using the JT gravity setup, we confirm that the wormhole phase disintegrates into two black hole system at finite charge density.

1.1 Summary of results

Below, we outline the key findings of our analysis.

In the present work, we cook up a theory of Einstein-Maxwell-dilaton gravity within the JT gravity framework that exhibits a first order phase transition between the charged wormhole solutions at low temperature and black hole solutions at high temperature and chemical potential. In particular, we explore the thermal properties of both these solutions. We observe that the regularised free energy density ($\mathcal{F}_{(wh)}^{reg}$) of the configuration is almost constant for sufficiently low temperatures ($T < T_0$) indicating the presence of a ‘‘gapped’’ phase in the dual SYK model [6] at finite density.

As the temperature increases, we notice that the total charge (Q) and chemical potential (μ) of the wormhole solution drops down to zero near the critical temperature ($T \sim T_0$). On top of it, the regularised free energy density ($\mathcal{F}_{(wh)}^{reg}$) of the wormhole phase is found to be constant for sufficiently low values of the chemical potential ($\mu \ll 1$). Combining these two facts together, one is therefore tempted to think about a transition from the low temperature complex SYK to a Majorana SYK phase at $T = T_0$.

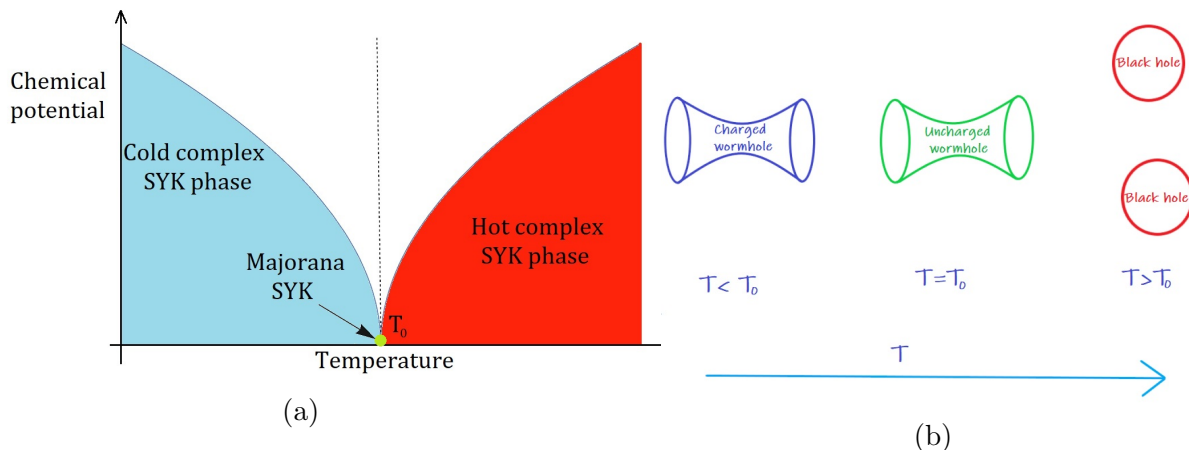


Figure 1: Figure (1a) represents the schematic plot of the chemical potential with temperature in SYK picture. On the other hand, figure (1b) illustrates the schematic phase structure in the dual gravity picture.

However, as the temperature is increased further beyond $T = T_0$, the charge density (as well as the chemical potential) starts increasing. We identify this as a transition from the Majorana SYK to a hot (complex) SYK phase at finite density (see figure (1a)).

Overall, we identify the above phenomena as a disintegration of the (Majorana) wormhole phase into a two (charged) black hole system.

The organisation for the rest of the paper is as follows. In Section 2, we set up the gravitational theory in two dimensions. In section 3, we construct the Euclidean wormhole solution in the presence of abelian one forms (A_μ) and compute the associated free energy. In section 4, we obtain the Euclidean black hole solution and estimate the corresponding free energy. In section 5, we explore the phase structure of the wormhole as well as the black hole solutions. Finally, in Section 6, we conclude our analysis by comparing it with the existing literature [6] and also comment on future directions associated to it.

2 Gravitational set up in 2D

We set up the theory of Einstein-dilaton gravity coupled with abelian ($U(1)$) one forms A_μ that exhibits a consistent wormhole solution in two dimensions.

We propose an action of the form

$$S_{JT} = \int d^2x \sqrt{-g} \left[\Phi(R + 2) + a_1 \Phi^{2n} F^2 + a_2 \Phi^n \varepsilon^{\mu\nu} F_{\mu\nu} + (\partial\chi)^2 \right] + \int d\tau \sqrt{-\gamma} \Phi 2K, \quad (2.1)$$

where n, a_1, a_2 are constants (those will be fixed latter on), Φ is the dilaton field and χ is a scalar field. Furthermore, here $\varepsilon^{\mu\nu} = \frac{1}{\sqrt{-g}} \epsilon^{\mu\nu}$ and K is the trace of extrinsic curvature.

The variation of the action (2.1) yields the following equations of motion

$$\Phi : (R + 2) + 2na_1 \Phi^{2n-1} F^2 + a_2 n \Phi^{n-1} \varepsilon^{\mu\nu} F_{\mu\nu} = 0, \quad (2.2)$$

$$\chi : \square\chi = 0, \quad (2.3)$$

$$A_\mu : \nabla_\mu [2a_1 \Phi^{2n} F^{\mu\nu} + a_2 \Phi^n \varepsilon^{\mu\nu}] = 0, \quad (2.4)$$

$$g_{\mu\nu} : \square\Phi g_{\mu\nu} - \nabla_\mu \nabla_\nu \Phi - g_{\mu\nu} \Phi + \langle T_{\mu\nu} \rangle = 0, \quad (2.5)$$

where $\langle T_{\mu\nu} \rangle$ is the full stress tensor² combining $U(1)$ gauge fields and the scalar field χ

$$\langle T_{\mu\nu} \rangle = \langle T_{\mu\nu}^{(gauge)} \rangle + \langle T_{\mu\nu}^{(\chi)} \rangle, \quad (2.6)$$

$$\langle T_{\mu\nu}^{(gauge)} \rangle = a_1 \Phi^{2n} \left[2g^{\alpha\beta} F_{\mu\alpha} F_{\nu\beta} - \frac{1}{2} F^2 g_{\mu\nu} \right], \quad (2.7)$$

$$\langle T_{\mu\nu}^{(\chi)} \rangle = (\partial_\mu \chi)(\partial_\nu \chi) - \frac{1}{2} g_{\mu\nu} (\partial\chi)^2. \quad (2.8)$$

It is interesting to notice that the equation of motion for the space-time metric $g_{\mu\nu}$ (2.5) allows both the wormhole as well as the blackhole solution. We study both of these solutions separately and establish a possible inter-transition at high temperatures.

3 Euclidean wormholes

We begin by considering the possibilities for an Euclidean wormhole solution of (2.1) whose geometry is described by the double trumpet [4] having two asymptotics. The corresponding space-time metric is expressed as

$$ds^2 = \frac{1}{\cos^2 \rho} (d\tau^2 + d\rho^2); \quad -\frac{\pi}{2} \leq \rho \leq \frac{\pi}{2}, \quad \tau \sim \tau + b, \quad (3.1)$$

²We define the stress tensor as $T_{\mu\nu} = \frac{1}{\sqrt{-g}} \frac{\delta S}{\delta g^{\mu\nu}}$.

where b is the periodicity of the Euclidean time (τ).

Given (3.1), we prefer to solve the equations of the motion (2.2)-(2.5) in the following static gauge

$$A_\tau = \xi(\rho), \quad A_\sigma = 0, \quad \Phi = \Phi(\rho), \quad \chi = \chi(\rho). \quad (3.2)$$

Using (3.1) and (3.2), it is now trivial to find

$$\chi = C_1 \rho + C_2, \quad (3.3)$$

where C_1 and C_2 are the integration constants³.

On the other hand, the equations of motion for Φ (2.2) and A_μ (2.4) can be reduced into a single equation of the form

$$\Phi^n \cos^2 \rho (\partial_\rho \xi) = \frac{a_2}{2a_1}, \quad (3.4)$$

Notice that, while arriving at (3.4), we set the integration constant (that arises from (2.4)) to be zero for the consistent wormhole solution.

3.1 Stress tensor

In the present section, we compute the full stress-energy tensor $\langle T_{\mu\nu} \rangle$ combining $U(1)$ gauge fields and the scalar field χ

$$\langle T_{\mu\nu} \rangle = \langle T_{\mu\nu}^{(gauge)} \rangle + \langle T_{\mu\nu}^{(\chi)} \rangle, \quad (3.5)$$

where $\langle T_{\mu\nu}^{(\chi)} \rangle$ denotes the stress tensor for the scalar field (χ) and $\langle T_{\mu\nu}^{(gauge)} \rangle$ corresponds to the stress tensor for $U(1)$ gauge fields (A_μ).

The general strategy would be to break the stress tensor (3.5) into classical and quantum pieces [4]

$$\begin{aligned} \langle T_{\mu\nu} \rangle_{cl} &= \langle T_{\mu\nu}^{(\chi)} \rangle_{cl} + \langle T_{\mu\nu}^{(gauge)} \rangle_{cl}, \\ \langle T_{\mu\nu} \rangle_{qm} &= \langle T_{\mu\nu}^{(\chi)} \rangle_{qm} + \langle T_{\mu\nu}^{(gauge)} \rangle_{qm}, \end{aligned} \quad (3.6)$$

where ‘cl’ stands for the classical and ‘qm’ stands for the quantum stress-energy tensor.

The classical part of the stress tensor can be computed directly using (3.1)-(3.3) in (2.7) and (2.8). On the other hand, we use the point-splitting method [4] to determine the quantum stress-energy tensor for gauge fields and the scalar field χ .

The classical and quantum stress-energy tensor for scalar field χ is quite straightforward to obtain [4]. These results can be summarised as

$$\langle T_{\rho\rho}^{(\chi)} \rangle_{cl} = - \langle T_{\tau\tau}^{(\chi)} \rangle_{cl} = \frac{C_1^2}{2}, \quad (3.7)$$

$$\begin{aligned} \langle T_{\rho\rho}^{(\chi)} \rangle_{qm} &= \frac{1}{24\pi} - \frac{1}{24\pi \cos^2 \rho} + X_{\rho\rho}(b), \\ X_{\rho\rho}(b) &= - \sum_{p \in \mathbb{Z}} \frac{p\pi}{b^2 \tanh(2\pi^2 p/b)}, \end{aligned} \quad (3.8)$$

$$\begin{aligned} \langle T_{\theta\theta}^{(\chi)} \rangle_{qm} &= - \frac{1}{24\pi} - \frac{1}{24\pi \cos^2 \rho} + X_{\theta\theta}(b), \\ X_{\theta\theta}(b) &= \sum_{p \in \mathbb{Z}} \frac{p\pi}{b^2 \tanh(2\pi^2 p/b)}. \end{aligned} \quad (3.9)$$

³Notice that C_1 is a complex constant [4].

The major part of the present computation involves estimating the stress-energy tensor for $U(1)$ gauge fields. The classical stress-energy tensor for $U(1)$ gauge fields can be obtained using (2.7) and (3.1)

$$\langle T_{\rho\rho}^{(gauge)} \rangle_{cl} = \langle T_{\tau\tau}^{(gauge)} \rangle_{cl} = a_1 \Phi^{2n} \cos^2 \rho (\partial_\rho \xi)^2. \quad (3.10)$$

Our next task is to compute the expectation value of the quantum stress-energy tensor [4] in the double trumpet background (3.1). Following [4], we first calculate the expectation value of the stress tensor in cylindrical coordinates using the point-splitting method and then perform the Weyl transformation.

Systematically, one can express the quantum expectation value as

$$\langle T_{\mu\nu}^{(gauge)} \rangle_{qm} = \langle T_{\mu\nu}^{(gauge)} \rangle_{qm} + \langle T_{\mu\nu}^{(gauge)} \rangle_{qm}, \quad (3.11)$$

where ‘*cyl*’ stands for the stress tensor in the cylindrical gauge and ‘*anm*’ stands for the anomalous part of the stress-energy tensor.

3.1.1 Cylindrical coordinates

We first calculate the stress-energy tensor in the cylindrical coordinates

$$ds^2 = d\theta^2 + d\rho^2; \quad -\frac{\pi}{2} \leq \rho \leq \frac{\pi}{2}, \quad \theta \sim \theta + b \quad \text{and} \quad A_\mu \equiv (A_\theta(\theta, \rho), 0), \quad (3.12)$$

where b is the periodicity in θ .

Notice that the equation of motion (2.4) in the cylindrical coordinates (3.12) leads to

$$\hat{\mathbf{F}}A_\theta = J(\rho), \quad (3.13)$$

where $\hat{\mathbf{F}} = \partial_\rho^2 + f(\rho)\partial_\rho$ is corresponding the differential operator.

Furthermore, here we define

$$f(\rho) = -2n(\partial_\rho \psi), \quad J(\rho) = -\frac{na_2}{2a_1} e^{n\psi} \partial_\rho \psi, \quad \Phi = e^{-\psi}.$$

In order to proceed further, we segregate out gauge field components from (2.1)

$$S_{gauge} = a_1 \int_{(I)} d^2x \sqrt{-g} \Phi^{2n} F^2 + a_2 \int_{(II)} d^2x \sqrt{-g} \Phi^n \varepsilon^{\mu\nu} F_{\mu\nu}. \quad (3.14)$$

Notice that, the variation of the second integral (*II*) with respect to the metric $g_{\mu\nu}$ vanishes. Therefore, only the first integral (*I*) contributes to the expectation value of the quantum stress-energy tensor (3.11).

In order to take the variation of (3.14), we decompose the (first) integral (*I*) into the bulk and the boundary, pieces

$$S_{gauge} = 2a_1 \int d^2x A_\nu \partial_\mu \left[\sqrt{-g} \Phi^{2n} K^{\mu\alpha\nu\beta} \partial_\beta A_\alpha \right] + a_2 \int d^2x \sqrt{-g} \Phi^n \varepsilon^{\mu\nu} F_{\mu\nu} + S_{boundary},$$

$$K^{\mu\alpha\nu\beta} = g^{\mu\alpha} g^{\nu\beta} - g^{\mu\beta} g^{\nu\alpha}, \quad (3.15)$$

and ignore the boundary contribution for obvious reasons.

The variation of (3.15) with respect to the bulk metric $g^{\eta\kappa}$ yields the following expression

$$\begin{aligned} \frac{\delta S_{gauge}}{\delta g^{\eta\kappa}} = & 2a_1 \int d^2x \left[A_\nu \left[\Phi^{2n} \left\{ -\frac{1}{2} \left(\partial_\mu (g_{\eta\kappa} \sqrt{-g}) + \sqrt{-g} g_{\lambda\sigma} \frac{\delta(\partial_\mu g^{\lambda\sigma})}{\delta g^{\eta\kappa}} \right) K^{\mu\alpha\nu\beta} - \right. \right. \right. \\ & \left. \left. \frac{1}{2} \sqrt{-g} g_{\eta\kappa} (\partial_\mu K^{\mu\alpha\nu\beta}) + \sqrt{-g} \left(g^{\nu\beta} \frac{\delta(\partial_\mu g^{\mu\alpha})}{\delta g^{\eta\kappa}} + g^{\mu\alpha} \frac{\delta(\partial_\mu g^{\nu\beta})}{\delta g^{\eta\kappa}} - g^{\nu\alpha} \frac{\delta(\partial_\mu g^{\mu\beta})}{\delta g^{\eta\kappa}} - g^{\mu\beta} \frac{\delta(\partial_\mu g^{\nu\alpha})}{\delta g^{\eta\kappa}} \right) \right\} \right] \\ & (\partial_\beta A_\alpha) + \Phi^{2n} \left\{ A_\nu (\partial_\eta \sqrt{-g}) g^{\nu\beta} \partial_\beta A_\kappa + A_\eta (\partial_\mu \sqrt{-g}) g^{\mu\alpha} \partial_\kappa A_\alpha - A_\nu (\partial_\eta \sqrt{-g}) g^{\nu\beta} \partial_\kappa A_\beta - \right. \\ & A_\eta (\partial_\mu \sqrt{-g}) g^{\mu\beta} \partial_\beta A_\kappa + \sqrt{-g} \left(A_\nu \partial_\eta (g^{\nu\beta}) \partial_\beta A_\kappa + A_\eta \partial_\mu (g^{\mu\alpha}) \partial_\kappa A_\alpha - A_\nu \partial_\eta (g^{\nu\alpha}) \partial_\kappa A_\alpha - \right. \\ & \left. \left. A_\eta \partial_\mu (g^{\mu\beta}) \partial_\beta A_\kappa \right) \right\} + \sqrt{-g} \left\{ A_\nu g^{\nu\beta} \partial_\eta (\Phi^{2n} \partial_\beta A_\kappa) - \frac{1}{2} A_\nu g_{\eta\kappa} K^{\mu\alpha\nu\beta} \partial_\mu (\Phi^{2n} \partial_\beta A_\alpha) + \right. \\ & \left. A_\eta g^{\mu\alpha} \partial_\mu (\Phi^{2n} \partial_\kappa A_\alpha) - A_\nu g^{\nu\alpha} \partial_\eta (\Phi^{2n} \partial_\kappa A_\alpha) - A_\eta g^{\mu\beta} \partial_\mu (\Phi^{2n} \partial_\beta A_\kappa) \right\} \right]. \end{aligned} \quad (3.16)$$

In the cylindrical coordinates (3.12), the above expression (3.16) further simplifies as

$$\frac{\delta S_{gauge}}{\delta g^{\theta\theta}} = \frac{\delta S_{gauge}}{\delta g^{\rho\rho}} = -a_1 \int d^2x A_\theta \hat{\mathbf{L}} A_\theta, \quad (3.17)$$

where $\hat{\mathbf{L}}$ is the differential operator such that $\hat{\mathbf{L}} A_\theta = \partial_\rho (\Phi^{2n} \partial_\rho A_\theta)$.

Using (3.17) as well as the point splitting method, the expectation value of the quantum stress-energy tensor⁴ turns out to be

$$\begin{aligned} \langle T_{\theta\theta}^{(gauge)} \rangle_{qm} = \langle T_{\rho\rho}^{(gauge)} \rangle_{qm} = & \frac{a_1}{2} \left[\lim_{x' \rightarrow x} \partial_\rho \left(\Phi^{2n}(\rho') \partial_{\rho'} G(\rho, \theta; \rho', \theta') \right) + \right. \\ & \left. \lim_{x \rightarrow x'} \partial_{\rho'} \left(\Phi^{2n}(\rho) \partial_\rho G(\rho, \theta; \rho', \theta') \right) \right], \end{aligned} \quad (3.18)$$

where $x \equiv (\rho, \theta)$, $x' \equiv (\rho', \theta')$.

Here $G(\rho, \theta; \rho', \theta')$ is the Green's function which satisfies the following equation

$$\hat{\mathbf{F}} G(\rho, \theta; \rho', \theta') = -\delta(\rho - \rho') \delta(\theta - \theta'), \quad (3.19)$$

where the operator $\hat{\mathbf{F}}$ is given by (3.13).

In order to solve (3.19), we consider the Fourier decomposition of $G(\rho, \theta; \rho', \theta')$ and $\delta(\theta - \theta')$

$$G(\rho, \theta; \rho', \theta') = \sum_{m, m' \in \mathbb{Z}} \tilde{G}(\rho, m; \rho', m') e^{2\pi i(m\theta + m'\theta')/b}, \quad (3.20)$$

$$\delta(\theta - \theta') = \frac{1}{b} \sum_{m, m' \in \mathbb{Z}} e^{2\pi i(m\theta + m'\theta')/b} \delta_{m+m'}, \quad (3.21)$$

and impose the following boundary conditions on $\tilde{G}(\rho, m; \rho', m')$

$$\tilde{G} \Big|_{\rho=\frac{\pi}{2}} = \tilde{G} \Big|_{\rho=-\frac{\pi}{2}} = 0. \quad (3.22)$$

⁴Notice that, there are two possible ways in which the differential operator $\hat{\mathbf{L}}$ can act on the Green's function $G(\rho, \theta; \rho', \theta')$. However, both the possibilities give the same result. Therefore, we consider the average of both the possibilities in the definition of the expectation value of the stress tensor.

On plugging (3.20) and (3.21) into (3.19), we obtain

$$\left[\partial_\rho^2 + f(\rho) \partial_\rho \right] \tilde{G}(\rho, m; \rho', m') = -\frac{1}{b} \delta(\rho - \rho') \delta_{m+m'}. \quad (3.23)$$

In addition to (3.22), \tilde{G} also satisfies the following properties :

- It is continuous in the limit $\rho \rightarrow \rho' : \tilde{G}(\rho) = \tilde{G}(\rho')$.
- Its derivative is discontinuous in the limit⁵ $\epsilon \rightarrow 0$ namely,

$$\left. \frac{d\tilde{G}}{d\rho} \right|_{\rho'+\epsilon} - \left. \frac{d\tilde{G}}{d\rho} \right|_{\rho'-\epsilon} = -\frac{1}{b}. \quad (3.24)$$

Notice that, $f(\rho)$ in (3.23) is an unknown function of ρ . Therefore one cannot solve (3.23) exactly for all values of ρ . However, we are interested in the near boundary analysis, therefore we solve (3.23) in the near boundary limits, $\rho \rightarrow \pm \frac{\pi}{2}$.

- Case 1 : $\rho \sim \rho_R \sim \frac{\pi}{2}$ and $-\frac{\pi}{2} < \rho' < \rho < \frac{\pi}{2}$
On expanding $f(\rho)$ near $\rho \sim \frac{\pi}{2}$, we find

$$f(\rho) \approx p_0 + p_1 \left(\rho - \frac{\pi}{2} \right), \quad \text{where } p_0 = f\left(\frac{\pi}{2}\right) \text{ and } p_1 = f'\left(\frac{\pi}{2}\right). \quad (3.25)$$

Furthermore, we set $m' = -m$ and plug (3.25) into (3.23) to obtain \tilde{G}

$$\begin{aligned} \tilde{G}_+(\rho, \rho', m) = & -\frac{1}{\sqrt{p_1}} \sqrt{\frac{\pi}{2}} \exp\left[\frac{1}{8p_1}(-2p_0 + \pi p_1)^2\right] \text{Erf}\left[\frac{1}{2\sqrt{2p_1}}(-2p_0 + (\pi - 2\rho)p_1)\right] A(\rho', m) \\ & + B(\rho', m), \end{aligned} \quad (3.26)$$

where the subscript ‘+’ denotes the value of Green’s function near the right boundary $\rho_R \sim +\frac{\pi}{2}$.

- Case 2 : $\rho \sim \rho_L \sim -\frac{\pi}{2}$ and $-\frac{\pi}{2} < \rho < \rho' < \frac{\pi}{2}$
On expanding $f(\rho)$ near $\rho \sim -\frac{\pi}{2}$, one finds

$$f(\rho) \approx q_0 + q_1 \left(\rho + \frac{\pi}{2} \right), \quad \text{where } q_0 = f\left(-\frac{\pi}{2}\right) \text{ and } q_1 = f'\left(-\frac{\pi}{2}\right). \quad (3.27)$$

Setting $m' = -m$ and plugging (3.27) back into (3.23), we find

$$\begin{aligned} \tilde{G}_-(\rho, \rho', m) = & \frac{1}{\sqrt{q_1}} \sqrt{\frac{\pi}{2}} \exp\left[\frac{1}{8q_1}(2q_0 + \pi q_1)^2\right] \text{Erf}\left[\frac{1}{2\sqrt{2q_1}}(2q_0 + (\pi + 2\rho)q_1)\right] C(\rho', m) \\ & + D(\rho', m), \end{aligned} \quad (3.28)$$

where the subscript ‘-’ denotes the value of Green’s function near the left boundary $\rho_L \sim -\frac{\pi}{2}$.

⁵Here, we integrate (3.23) with respect to ρ from $\rho = \rho' - \epsilon$ to $\rho = \rho' + \epsilon$ and take the limit $\epsilon \rightarrow 0$.

One can further solve the functions $A(\rho', m)$, $B(\rho', m)$, $C(\rho', m)$ and $D(\rho', m)$ using the boundary conditions (3.22) and (3.24). Finally, (3.20) can be systematically expressed as

$$G(\rho, \theta; \rho', \theta') = \begin{cases} \sum_{m \in \mathbb{Z}} G_+(\rho, \theta; \rho', \theta', m) & -\frac{\pi}{2} < \rho' < \rho < \frac{\pi}{2} \\ \sum_{m \in \mathbb{Z}} G_-(\rho, \theta; \rho', \theta', m) & -\frac{\pi}{2} < \rho < \rho' < \frac{\pi}{2} \end{cases}, \quad (3.29)$$

where the detailed expressions of G_{\pm} are given in the Appendix A.

Finally, plugging (3.29) into (3.18) and retaining terms only upto leading order in an expansion near the boundaries one finds

$$\begin{aligned} \langle T_{\theta\theta}^{(gauge)} \rangle_{qm} = \langle T_{\rho\rho}^{(gauge)} \rangle_{qm} &= \frac{a_1}{b} \left(-p_0 + \frac{\exp\{-(q_0 + \pi q_1)^2/(2q_1)\} \sqrt{2q_1/\pi}}{\text{Erf}\left[\frac{q_0}{\sqrt{2q_1}}\right] - \text{Erf}\left[\frac{q_0 + \pi q_1}{\sqrt{2q_1}}\right]} \right) \Phi\left(\frac{\pi}{2}\right)^{2n} \\ &+ O\left(\rho - \frac{\pi}{2}\right)^1, \end{aligned} \quad (3.30)$$

$$\begin{aligned} \langle T_{\theta\theta}^{(gauge)} \rangle_{qm} = \langle T_{\rho\rho}^{(gauge)} \rangle_{qm} &= \frac{a_1}{b} \left(q_0 + \frac{\exp\{-(p_0 - \pi p_1)^2/(2p_1)\} \sqrt{2p_1/\pi}}{-\text{Erf}\left[\frac{p_0}{\sqrt{2p_1}}\right] + \text{Erf}\left[\frac{p_0 - \pi p_1}{\sqrt{2p_1}}\right]} \right) \Phi\left(-\frac{\pi}{2}\right)^{2n} \\ &+ O\left(\rho + \frac{\pi}{2}\right)^1, \end{aligned} \quad (3.31)$$

where the subscript ‘ \pm ’ denotes the expectation value of the quantum stress-energy tensor near the boundary $\rho = \pm \frac{\pi}{2}$.

3.1.2 Weyl anomaly

We now calculate the contributions due to the presence of the Weyl anomaly [25]. One can estimate the Weyl anomaly using the transformation properties of the stress-energy tensor (3.11) under the Weyl transformation

$$g_{\mu\nu}^{(cyl)} \rightarrow g_{\mu\nu}^{(W)} = e^{2\sigma(x)} g_{\mu\nu}^{(cyl)}. \quad (3.32)$$

The corresponding stress-energy tensor transforms⁶ [25] as

$$\frac{\delta}{\delta\sigma(x')} \left(\sqrt{-g^{(W)}(x)} \langle T_{\nu}^{\mu}(x) \rangle \right) = 2g_{\gamma\nu}^{(W)}(x) \frac{\delta}{\delta g_{\mu\gamma}^{(W)}(x)} \left(\sqrt{-g^{(W)}(x')} \langle T_{\alpha}^{\alpha}(x') \rangle \right). \quad (3.33)$$

The variation of the quantum stress-energy tensor with respect to the conformal factor can be evaluated taking the trace of (2.7)

$$g^{\mu\nu} \langle T_{\mu\nu}^{(gauge)} \rangle = a_1 \Phi^{2n} F^2. \quad (3.34)$$

Treating $x' = x$ and solving (3.33) in the gauge (3.1) along with (3.34) we find

$$\frac{1}{\tan \rho} \frac{d}{d\rho} \left(\frac{1}{\cos^2 \rho} \langle T_{\rho}^{\rho} \rangle \right) = -4a_1 \Phi^{2n} \cos^2 \rho (\partial_{\rho} \xi)^2, \quad (3.35)$$

⁶See Appendix B for the details of the derivation.

where we identify $e^{-2\sigma} = \cos^2 \rho$.

The quantum anomalous stress tensor for the gauge fields can be evaluated using the equation of constraint (3.4) in (3.35), which yields

$$\langle T_{\rho\rho}^{(gauge)} \rangle_{qm} = \langle T_{\tau\tau}^{(gauge)} \rangle_{qm} = C_3 - \frac{a_2^2}{2a_1 \cos^2 \rho}, \quad (3.36)$$

where C_3 is the integration constant.

Substituting (3.7)-(3.9), (3.10), (3.30), (3.31) and (3.36) into (3.5) one finally obtains the full stress-energy tensor combining $U(1)$ gauge fields and the scalar field χ . In the next section, we use this piece of information to calculate the profile for the dilaton field in the asymptotic limits ($\rho \rightarrow \pm \frac{\pi}{2}$).

3.2 Solving for Φ and ξ

Before we proceed further, let us first calculate the boundary stress tensor⁷ using the Gibbons-Hawking-York term (2.1)

$$T_{\tau\tau} \Big|_{boundary} = \frac{1}{\sqrt{-\gamma}} \frac{\delta S_{GHY}}{\delta \gamma^{\tau\tau}}, \text{ where } S_{GHY} = \int d\tau \sqrt{-\gamma} \Phi 2K, \quad (3.37)$$

which plays the crucial role in obtaining the near boundary profile of the dilaton (Φ).

On solving (3.37) in the double trumpet geometry (3.1) one finds

$$T_{\tau\tau} \Big|_+ = \alpha \Phi \sec \rho \tan \rho \text{ and } T_{\tau\tau} \Big|_- = \beta \Phi \sec \rho \tan \rho, \quad (3.38)$$

where the subscripts \pm denotes the boundary stress tensor near the asymptotic limits $\rho_{L,R} \sim \pm \frac{\pi}{2}$ and α, β are constants.

Given the double trumpet geometry (3.1), the equation of motion for $g_{\mu\nu}$ (2.5) turns out to be

$$\partial_\rho^2 \Phi - \tan \rho \partial_\rho \Phi - \frac{\Phi}{\cos^2 \rho} + \langle T_{\tau\tau} \rangle = 0, \quad (3.39)$$

where $\langle T_{\tau\tau} \rangle = \langle T_{\tau\tau}^{(gauge)} \rangle + \langle T_{\tau\tau}^{(scalar)} \rangle + \langle T_{\tau\tau}^{(boundary)} \rangle$.

Upon solving equation (3.39) one finds the following asymptotic profiles

$$\Phi_+ = \frac{-F_+}{\left(\frac{\pi}{2} - \rho\right)} - \frac{1}{24\pi} - \frac{a_2^2}{2a_1} + \alpha r_0 \text{ and } \Phi_- = \frac{F_-}{\left(\rho + \frac{\pi}{2}\right)} - \frac{1}{24\pi} - \frac{a_2^2}{2a_1} - \beta s_0, \quad (3.40)$$

where the subscripts ‘ \pm ’ denote the leading order terms in Φ .

⁷A similar calculation is also discussed in [26].

The functions F_{\pm} on the other hand, are given by

$$F_+ = \frac{\pi}{2} \left(-\frac{1}{18\pi} - \frac{a_2^2}{6a_1} - \frac{C_1^2}{2} + C_3 + \frac{a_1}{b} \left(-p_0 + \frac{\exp\{-(q_0 + \pi q_1)^2/(2q_1)\} \sqrt{2q_1/\pi}}{\text{Erf}\left[\frac{q_0}{\sqrt{2q_1}}\right] - \text{Erf}\left[\frac{q_0 + \pi q_1}{\sqrt{2q_1}}\right]}\right) r_0^2 - \frac{1}{6} \alpha(r_0 - 3r_2) + X_{\theta\theta}(b) \right) - C_4 + 0.1159\alpha r_1, \quad (3.41)$$

$$F_- = -\frac{\pi}{2} \left(-\frac{1}{18\pi} - \frac{a_2^2}{6a_1} - \frac{C_1^2}{2} + C_3 + \frac{a_1}{b} \left(q_0 + \frac{\exp\{-(p_0 - \pi p_1)^2/(2p_1)\} \sqrt{2p_1/\pi}}{-\text{Erf}\left[\frac{p_0}{\sqrt{2p_1}}\right] + \text{Erf}\left[\frac{p_0 - \pi p_1}{\sqrt{2p_1}}\right]}\right) s_0^2 + \frac{1}{6} \beta(s_0 - 3s_2) + X_{\theta\theta}(b) \right) + C_5 - 0.1159\beta s_1, \quad (3.42)$$

where $r_0 = \Phi\big|_{\rho=\frac{\pi}{2}}$, $r_1 = \Phi'\big|_{\rho=\frac{\pi}{2}}$, $r_2 = \Phi''\big|_{\rho=\frac{\pi}{2}}$, $s_0 = \Phi\big|_{\rho=-\frac{\pi}{2}}$, $s_1 = \Phi'\big|_{\rho=-\frac{\pi}{2}}$, $s_2 = \Phi''\big|_{\rho=-\frac{\pi}{2}}$ and C_4, C_5 are the integration constants.

Using (3.4) and (3.40), the asymptotic profile of the gauge field turns out to be

$$\xi_{\pm} = -\frac{2a}{F_{\pm}} \log\left(\rho \mp \frac{\pi}{2}\right) + \mu_{\pm}, \quad (3.43)$$

where μ_{\pm} denote the chemical potentials⁸ near the asymptotic boundaries $\rho_{L,R} \sim \pm\frac{\pi}{2}$

$$\mu_+ = \frac{\pi a r_2}{6\alpha r_0^2} \log\left(\frac{3}{2}\pi^2 \alpha r_2\right) \quad \text{and} \quad \mu_- = \frac{\pi a s_2}{6\beta s_0^2} \log\left(\frac{3}{2}\pi^2 \beta s_2\right). \quad (3.44)$$

3.3 Thermodynamics of wormholes

We now examine the thermal properties of the Euclidean wormhole solution obtained in (3.1). In particular from the periodicity of the Euclidean time (τ), we identify the temperature (T) of the wormhole solution near the asymptotics ($\rho_{L,R}$) and compute its free energy. We also compute the total charge associated with the wormhole solution and look at its variation with temperature.

3.3.1 Temperature

In order to determine the temperature of the wormhole, we impose the following boundary conditions [4] on Φ and $g_{\mu\nu}$

$$\Phi \sim \frac{\phi}{\epsilon} \quad \text{and} \quad ds^2\bigg|_{\rho \rightarrow \pm\frac{\pi}{2}} \sim \frac{du_{\pm}^2}{\epsilon^2}, \quad (3.45)$$

where u_{\pm} are identical to τ and with the periodicity conditions $u_{\pm} \sim u_{\pm} + \phi\beta_{\pm}$. Here, β_{\pm} correspond to the inverse temperatures near the asymptotics $\rho_{L,R} = \pm\frac{\pi}{2}$.

Finally, using (3.1), (3.40) and (3.45), we identify the temperature associated with the wormhole solution near the asymptotics as

$$T_{\pm} = \mp \frac{F_{\pm}}{b}, \quad (3.46)$$

⁸We set $n = 1$, $a_1 = -\frac{1}{4}$ and $a_2 = a$.

where F_{\pm} are given in (3.41) and (3.42).

Notice that, the right temperature (T_+) of the wormhole near $\rho_R \sim \frac{\pi}{2}$ is different from that of the left temperature (T_-) near $\rho_L = -\frac{\pi}{2}$. However, setting $\beta = -\alpha$, $C_4 = C_5 = \eta$, $q_0 = -p_0$, $q_1 = p_1$, $s_0 = r_0$, $s_1 = -r_1$, $s_2 = r_2$ and $\mu_+ = -\mu_- = \mu$, we find that $T_+ \approx T_- = T$, where

$$T = \frac{1}{b} \left[\eta - 0.1159\alpha r_1 - \frac{\pi}{2} \left(-\frac{1}{18\pi} + \frac{2}{3} \left(\frac{6\mu\alpha r_0^2}{\pi r_2 \log(3\pi^2\alpha r_2/2)} \right)^2 - \frac{C_1^2}{2} + C_3 - \frac{r_0^2}{4b} \left(-p_0 + \frac{\exp\{-(q_0 + \pi q_1)^2/(2q_1)\} \sqrt{2q_1/\pi}}{\text{Erf}\left[\frac{q_0}{\sqrt{2q_1}}\right] - \text{Erf}\left[\frac{q_0 + \pi q_1}{\sqrt{2q_1}}\right]} \right) - \frac{1}{6}\alpha(r_0 - 3r_2) + X_{\theta\theta}(b) \right) \right]. \quad (3.47)$$

On reverting the above expression (3.47), we obtain the chemical potential (μ) in terms of the temperature (T)

$$\mu = \frac{0.51}{\alpha\sqrt{b}r_0^2} r_2 \log(14.80\alpha r_2) \left\{ b(0.02 - bT + \eta) + 0.78bC_1^2 - 1.57bC_3 + 0.26b\alpha r_0 - 0.39p_0r_0^2 - 0.11b\alpha r_1 - 0.78b\alpha r_2 - 1.57bX_{\theta\theta}(b) + \frac{\exp\{-0.5(q_0 + \pi q_1)^2/q_1\} 0.31\sqrt{q_1}r_0^2}{\text{Erf}\left[\frac{0.70q_0}{\sqrt{q_1}}\right] - \text{Erf}\left[\frac{0.70(q_0 + \pi q_1)}{\sqrt{q_1}}\right]} \right\}^{\frac{1}{2}}. \quad (3.48)$$

In a compact notation, one can express (3.48) as

$$\mu = \begin{cases} f\sqrt{T_0 - T} & T > T_0, \\ f\sqrt{T - T_0} & T < T_0, \end{cases} \quad (3.49)$$

where we identify the critical point of the first order phase transition as

$$T_0 = \frac{1}{b^2} \left\{ 0.02b + \eta b + 0.78bC_1^2 - 1.57bC_3 + 0.26b\alpha r_0 - 0.39p_0r_0^2 - 0.11b\alpha r_1 - 0.78b\alpha r_2 - 1.57bX_{\theta\theta}(b) + \frac{\exp\{-0.5(q_0 + \pi q_1)^2/q_1\} 0.31\sqrt{q_1}r_0^2}{\text{Erf}\left[\frac{0.70q_0}{\sqrt{q_1}}\right] - \text{Erf}\left[\frac{0.70(q_0 + \pi q_1)}{\sqrt{q_1}}\right]} \right\}, \quad (3.50)$$

together with the function, $f = \frac{0.51}{\alpha r_0^2} \sqrt{b} r_2 \log(14.80\alpha r_2)$.

3.3.2 Free energy

Our next task would be to compute the free energy (F) of the Euclidean wormhole solution (2.1). The free energy [27] of the wormhole solution is defined through the Euclidean partition function (Z)

$$F_{(wh)} = -\beta^{-1} \log Z, \quad Z = e^{-S_{(wh)}^{(os)}}, \quad (3.51)$$

where $S_{(wh)}^{(os)}$ stands for the onshell action of the wormhole.

Recall that, in Section 3.2, we determine Φ (3.40) near the asymptotic limits $\rho_{L,R} \rightarrow \pm \frac{\pi}{2}$. Using these asymptotic expressions for Φ , one can therefore calculate the free energy density of the wormhole solution (2.1) in the near boundary limits.

The free energy density (\mathcal{F}) of the wormhole solution is defined through the following integral of the form

$$F_{(wh)} = \int d\rho \mathcal{F}_{(wh)}. \quad (3.52)$$

Notice that, if we directly substitute (3.40) and (3.43) into (3.52), then $\mathcal{F}_{(wh)}$ diverges near the boundaries $\rho_{L,R} \sim \pm \frac{\pi}{2}$. Therefore, we define the ‘‘regularised’’ free energy density

$$\mathcal{F}_{wh}^{reg} = \mathcal{F}_{wh} + \mathcal{F}_{wh}^{ct}, \quad (3.53)$$

where the divergent piece is absorbed into the following counter term

$$\begin{aligned} \mathcal{F}_{(wh)}^{ct} = & -\frac{1}{\delta^2} \left(\frac{1}{18} + 2\eta + \frac{\pi C_1^2}{2} - \pi C_3 + \frac{1}{4b} \left(-\pi p_0 + \frac{\exp\{-(q_0 + \pi q_1)^2/(2q_1)\} \sqrt{2q_1\pi}}{\text{Erf}\left[\frac{q_0}{\sqrt{2q_1}}\right] - \text{Erf}\left[\frac{q_0 + \pi q_1}{\sqrt{2q_1}}\right]} \right) r_0^2 \right. \\ & - 0.231\alpha r_1 - 2\delta \left(-\frac{1}{24\pi} + \alpha r_0 + \frac{72\alpha^2 \mu^2 r_0^4}{\pi^2 \log(3\pi^2 \alpha r_2/2)^2 r_2^2} \right) + \frac{1}{6}\pi\alpha(r_0 - 3r_2) - \\ & \left. \pi X_{\theta\theta}(b) + \frac{72\alpha^2 \mu^2 r_0^4}{\pi^2 \log(3\pi^2 \alpha r_2/2)^2 r_2^2} - \frac{24\alpha^2 \mu^2 r_0^4}{\pi \log(3\pi^2 \alpha r_2/2)^2 r_2^2} \right), \end{aligned} \quad (3.54)$$

where δ acts as the UV cutoff of the theory.

Upon regularisation, the finite piece in the free energy⁹ turns out to be

$$\mathcal{F}_{(wh)}^{reg} = \begin{cases} C_1^2 - 1.303b(T - T_0) - \frac{2bT_0}{3} + \frac{6.966(T-T_0)T_0^2 b^2}{bT^2} \left(\frac{T}{T_0} - 1\right)^2 & T > T_0, \\ C_1^2 + 1.303b(T - T_0) - \frac{2bT_0}{3} - \frac{6.966(T-T_0)T_0^2 b}{(T-2T_0)^2} & T < T_0, \end{cases} \quad (3.55)$$

where we consider $T_0 \approx O(r_2)$ and $\left|\frac{r_0}{T_0}\right| \ll 1$.

It is interesting to notice that for the regularised free energy

$$\left. \frac{d\mathcal{F}_{T>T_0}^{(wh)}}{dT} \right|_{T=T_0} \neq \left. \frac{d\mathcal{F}_{T<T_0}^{(wh)}}{dT} \right|_{T=T_0}, \quad (3.56)$$

which clearly indicates the onset of a first order phase transition at $T = T_0$. We will shed some more light on the associated phase diagram in Section 5.

3.3.3 Charge

The total charge (Q) associated with the wormhole solutions turns out to be

$$Q = \frac{1}{4\pi} \int d\tau \sqrt{-\gamma} \varepsilon^{\mu\nu} F_{\mu\nu} \Big|_{\rho \sim \frac{\pi}{2}}. \quad (3.57)$$

⁹In this section, we compute $\mathcal{F}_{(wh)}$ near the right boundary, $\rho_R \sim \frac{\pi}{2}$. Finally, we notice that the finite piece of $\mathcal{F}_{(wh)}$ turns out to be the same in both the boundary limits i.e. $\mathcal{F}_{(wh)}^{reg} \Big|_{\rho_L \sim -\frac{\pi}{2}} = \mathcal{F}_{(wh)}^{reg} \Big|_{\rho_R \sim \frac{\pi}{2}}$.

Using (3.40), (3.43) and (3.49), we finally obtain

$$Q = \begin{cases} \frac{0.311054\sqrt{T_0-T}}{\sqrt{6}T^2} & T > T_0, \\ -\frac{0.31105\sqrt{T-T_0}}{\sqrt{6}(T^2-2TT_0)} & T < T_0. \end{cases} \quad (3.58)$$

4 Euclidean black holes

The purpose of this section is to construct the Euclidean black hole solution corresponding to (2.1). We further use these solutions to discuss the thermal properties of the solution.

We solve the equations of motion (2.2)-(2.5) ‘‘perturbatively’’ treating the couplings a_1, a_2 as an expansion parameter. Using static gauge, background fields are expressed as

$$\begin{aligned} ds^2 &= e^{2\omega(z)}(d\tau^2 + dz^2), \\ A_\mu &\equiv (A_\tau(z), 0), \quad \Phi = \Phi(z), \quad \chi = \chi(z). \end{aligned} \quad (4.1)$$

We expand background fields as [27]

$$\mathcal{A} = \mathcal{A}_0 + a_1\mathcal{A}_1 + a_2\mathcal{A}_2, \quad |a_1| \ll 1, \quad |a_2| \ll 1, \quad (4.2)$$

where \mathcal{A} stands for any of the fields ω, Φ, A_τ and χ .

Here the subscript ‘0’ stands for the pure JT gravity solution and the other two subscripts ‘1’ and ‘2’ denote the associated corrections due to $U(1)$ gauge fields [27]. In the following sections, we plug this expansion (4.2) into the equations of motion (2.2)-(2.5) and solve them at different order in the coupling.

4.1 Zeroth order solutions

Zeroth order solutions are obtained by setting the expansion parameters $a_1 = a_2 = 0$. The corresponding equations of motion (2.2)-(2.5) turns out to be

$$\Phi_0'' - 2e^{2\omega_0}\Phi_0 = 0, \quad (4.3)$$

$$\omega_0'' - e^{2\omega_0} = 0, \quad (4.4)$$

$$\chi_0'' = 0. \quad (4.5)$$

On solving (4.3)-(4.5), we find zeroth order solutions as

$$\omega_0 = \frac{1}{2} \log \left(\frac{4\rho_H}{\sinh^2(2\sqrt{\rho_H}z)} \right), \quad \Phi_0 = \sqrt{\rho_H} \coth(2\sqrt{\rho_H}z), \quad \chi_0 = b_1z + b_2, \quad (4.6)$$

where ρ_H, b_1 and b_2 are integration constants.

4.2 First order solutions

We now estimate the leading order contributions due to $U(1)$ gauge fields. The corresponding equations of motion (2.2)-(2.5) turn out to be

$$\Phi_1'' - 2(\omega_1'\Phi_0' + \omega_0'\Phi_1') - 2\chi_0'\chi_1' = 0, \quad (4.7)$$

$$\omega_1'' - 2\omega_0''\omega_1 - 2\Phi_0e^{-2\omega_0}A_{\tau 1}'^2 = 0, \quad (4.8)$$

$$\partial_z(\Phi_0^2e^{-2\omega_0}A_{\tau 1}') = 0, \quad (4.9)$$

$$\chi_1'' - 2\chi_0''\omega_1 = 0. \quad (4.10)$$

In order to solve (4.7)-(4.10), we adopt the following change in coordinates

$$z = \frac{1}{2\sqrt{\rho_H}} \coth^{-1} \left(\frac{\rho}{\sqrt{\rho_H}} \right), \quad (4.11)$$

where ρ_H denotes the location of the horizon.

Upon solving (4.7)-(4.10) we find first order corrections to the background fields

$$A_{\tau 1} = \frac{2b_3}{\rho} + b_4, \quad (4.12)$$

$$\begin{aligned} \omega_1 = & -\frac{b_3^2}{\rho_H^2 \rho} \left(\rho_H + \rho^2 (-2 \log(\rho) + \log(-\sqrt{\rho_H} + \rho) + \log(\sqrt{\rho_H} + \rho)) \right) - b_6 + \\ & \frac{\rho}{\sqrt{\rho_H}} \left(b_5 + \tanh^{-1} \left(\frac{\rho}{\sqrt{\rho_H}} \right) b_6 \right), \end{aligned} \quad (4.13)$$

$$\chi_1 = \frac{b_7}{\sqrt{\rho_H}} \tanh^{-1} \left(\frac{\rho}{\sqrt{\rho_H}} \right) + b_8, \quad (4.14)$$

$$\begin{aligned} \Phi_1 = & \frac{b_3^2}{\rho_H^2} \left((-\rho_H + \rho^2) (2 \log \rho - \log(-\sqrt{\rho_H} + \rho) - \log(\sqrt{\rho_H} + \rho)) \right) + \frac{1}{8\rho_H^{\frac{3}{2}}} \left(8\rho_H \rho^2 b_5 + \right. \\ & 4\rho_H \left(2\sqrt{\rho_H} \rho + 2\rho^2 \tanh^{-1} \left(\frac{\rho}{\sqrt{\rho_H}} \right) + \rho_H \log(-\sqrt{\rho_H} + \rho) - \rho_H \log(\sqrt{\rho_H} + \rho) \right) b_6 + \\ & \left. \rho \left(-\log(-\sqrt{\rho_H} + \rho) + \log(\sqrt{\rho_H} + \rho) \right) b_1 b_7 \right) + b_9 + \rho b_{10}, \end{aligned} \quad (4.15)$$

where b_3, b_4, \dots, b_{10} are the integration constants.

It is interesting to notice that when we compare the coefficient of a_2 in (2.4) we find

$$\partial_z \Phi_0 = 0 \Rightarrow \Phi_0 = \text{constant}, \quad (4.16)$$

which is clearly in conflict with (4.6). Therefore, the coefficient a_2 in (2.1) must be zero for the black hole phase. However, on the other hand, the coefficient a_2 plays a significant role in obtaining the consistent wormhole solution.

Finally, the space-time metric for the Euclidean black hole (4.1) turns out to be

$$ds^2 \approx 4(\rho^2 - \rho_H) (1 + 2a_1 \omega_1) \left(d\tau^2 + \frac{d\rho^2}{4(\rho_H - \rho^2)^2} \right), \quad (4.17)$$

where ω_1 is given by (4.13) and the black hole horizon is located at $\rho = \sqrt{\rho_H}$.

4.3 Black hole thermodynamics

We now explore the thermal properties of the Euclidean black hole solution obtained in the previous section. In particular, we obtain the Hawking temperature of the black hole and compute the associated free energy density.

The Hawking temperature¹⁰ of the 2D black hole [26] is given by

$$T_H = \frac{1}{2\pi} \sqrt{\frac{1}{4} g^{\tau\tau} g^{\rho\rho} (\partial_\rho g_{\tau\tau})^2} \Big|_{\rho \rightarrow \sqrt{\rho_H}} = \frac{\sqrt{\rho_H}}{\pi}. \quad (4.18)$$

Next, we compute the free energy of the Euclidean black hole solution (4.17). Like before, the free energy of the black hole solution is given by [27]

$$F_{(bh)} = -\beta^{-1} \log Z, \quad Z = e^{-S_{(bh)}^{(os)}}, \quad (4.19)$$

where $S_{(bh)}^{(os)}$ correspond to the Euclidean on-shell action for the black hole.

We define the “regularised” free energy of the black hole

$$F_{(bh)}^{reg} = F_{(bh)} + F_{(bh)}^{ct}, \quad (4.20)$$

where the divergences are absorbed in the following counter term

$$F_{(bh)}^{ct} = - \left(4\rho^2 - \frac{1}{4\sqrt{\rho_H}} \left(\log(\delta) b_1 (b_1 + 2a_1 b_7) \right) + \frac{\rho a_1}{\rho_H} \left(4b_3^2 - 4\sqrt{\rho_H} (\rho_H - 2\rho^2) b_5 + \right. \right. \\ \left. \left. 2\rho_H \left(4\rho + \pi \sqrt{-\frac{1}{\rho_H}} (\rho_H - 2\rho^2) \right) b_6 + b_1 b_7 + 4\rho_H (b_9 + \rho b_{10}) \right) \right), \quad (4.21)$$

where we set the limits as $\delta \rightarrow 0$ and $\rho \rightarrow \infty$.

Using (4.6) and (4.12)-(4.15) the regularised free energy finally turns out to be

$$F_{(bh)}^{reg} = \frac{5}{6} \pi^2 T^2 b_6 + \frac{b_1}{16\pi T} \left(2\pi + \log(4\pi^2 T^2) \right) (2b_1 - b_7), \quad (4.22)$$

where we retain only leading order terms in the near boundary ($\rho \rightarrow \infty$) expansion.

5 Phase transition

Finally, with all these solutions at hand, we explore the stability of the Euclidean wormhole solution (3.40)-(3.43) at high temperatures. The key observable in this regard are the regularised free energies (3.55) and (4.22) obtained previously.

The variation of the regularised free energy (3.55) with temperature is shown in figure (2). As the plots (in figure (2)) reveal, for sufficiently low temperatures¹¹ ($T \ll T_0$), the regularised free energy ($\mathcal{F}_{(wh)}^{reg}$) of the charged wormhole solution remains as a constant indicating the presence of a “gapped” phase in the two-site (complex) SYK model at finite density [6].

¹⁰In order to be consistent with [26], we set the constraint on constants b_3 and b_6 such that $2b_3^2 + \mu^{\frac{3}{2}} b_6 = 0$ with $b_6 < 0$.

¹¹Notice that, the critical temperature (T_0) of the solution contains several infinitely large constants (r_0, r_1 and r_2) which make the critical temperature (T_0) also a large quantity. For our purpose, we set the critical temperature $T_0 = 10^4$ and $b = 10^{-4}$ which therefore denotes the “small” wormhole solution [4].

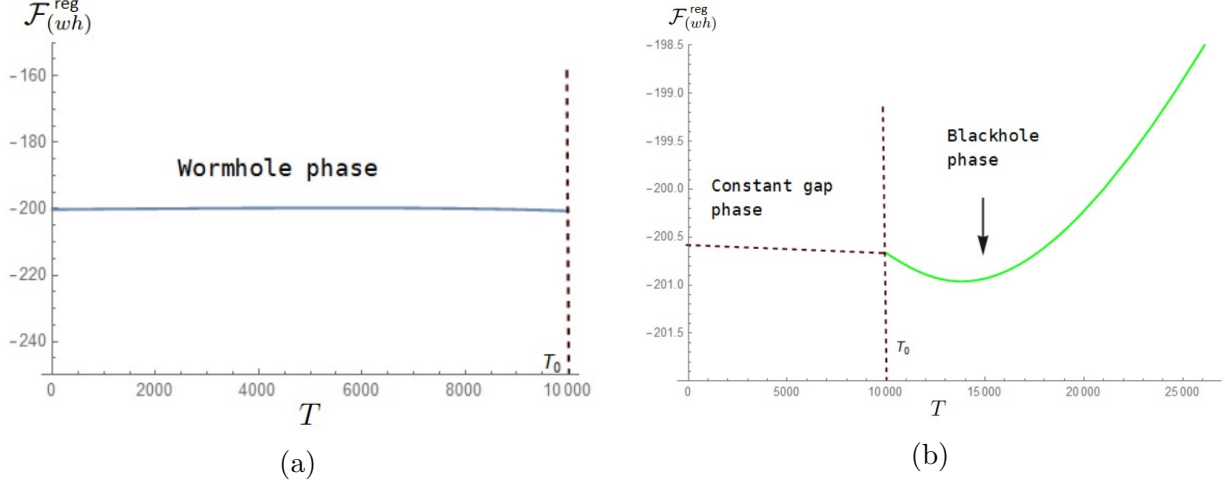


Figure 2: Plot of regularised free energy density ($\mathcal{F}_{(wh)}^{reg}$) with temperature (T).

As the temperature of the wormhole phase is further increased, we observe a “kink” (see figure (2)) at $T = T_0$ characterising a first order phase transition [4, 6].

On increasing the temperature further beyond $T = T_0$, the wormhole phase becomes unstable and passes over to the Euclidean (two) black hole phase (4.22) as shown in figure (2b). This claim is further solidified by identifying the behaviour of the regularised free energy of the black hole solution ($F_{(bh)}^{reg}$) (4.22) with temperature.

Therefore, to summarise, we conclude that at the critical temperature ($T \sim T_0$) the wormhole phase converts into the charged black hole phase via a first order phase transition. This new phase of the system (for $T > T_0$) is conjectured to be dual to a hot (two-site) SYK model at finite density.

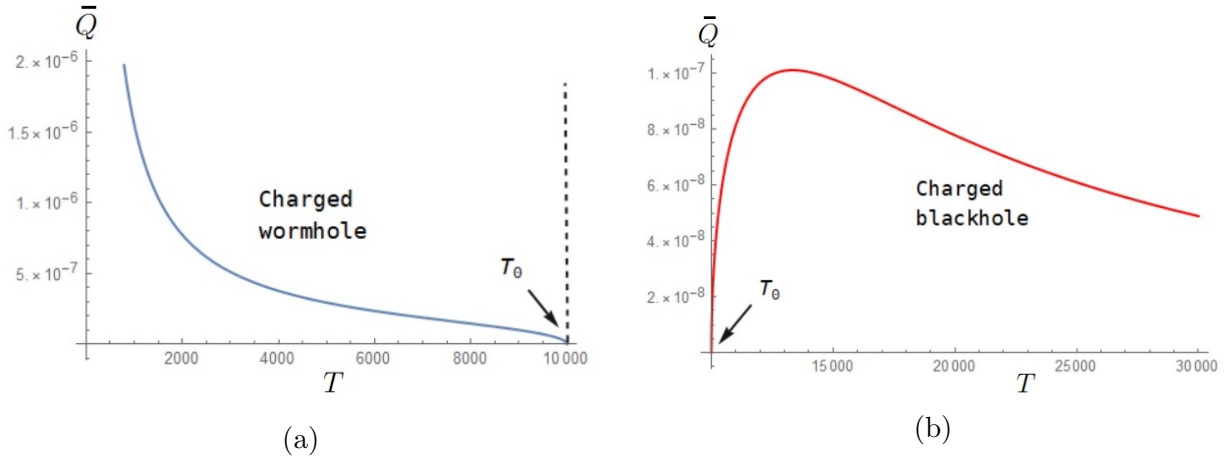
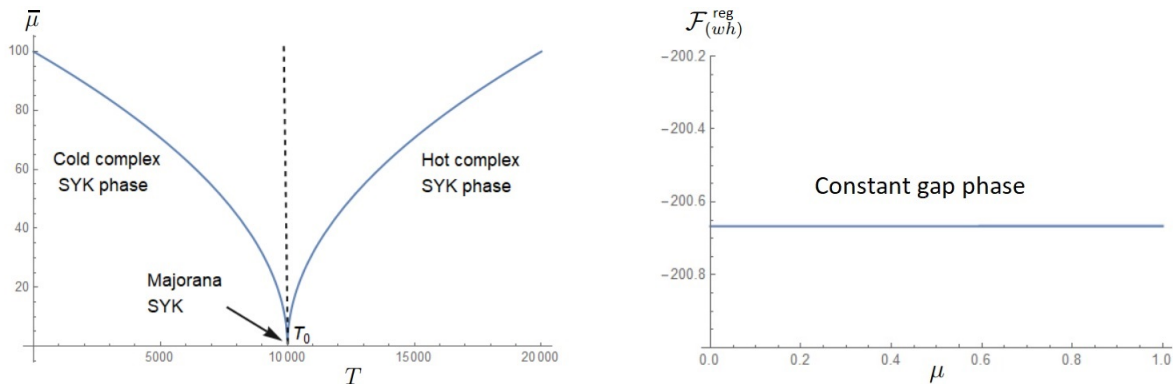


Figure 3: Plot of re-scaled total charge (\bar{Q}) with temperature T , where $\bar{Q} = Q\sqrt{b}$.

We also plot the total charge (Q) (3.58) as well as the chemical potential (μ) (3.49) as a function of the temperature (T) (see figure (3) and (4a) respectively) which reveal further information associated with the phase diagram. Notice that, in the vicinity of the critical temperature ($T \sim T_0$), the total charge (Q) and the chemical potential (μ) of the wormhole solution becomes significantly small and in fact vanishes exactly at the critical point, $T = T_0$ (see figure 3b). Therefore, at the critical point, the complex SYK switches

over to a (two site) Majorana SYK phase [4] which eventually acts as a glue between the cold ($T < T_0$) and the hot ($T > T_0$) SYK phases (see figure 4a) lying in two different temperature regimes.



(a) Chemical potential *vs.* temperature (b) Free energy density *vs.* chemical potential

Figure 4: In figure (4a), we plot the re-scaled chemical potential ($\bar{\mu}$) with temperature where $\bar{\mu} = \mu/f$. Figure (4b) represents the plot of the regularised free energy density of the wormhole solution with chemical potential (μ).

We further confirm that the Majorana phase ($\mu \sim Q \sim 0$) at $T = T_0$ corresponds to a (uncharged) wormhole solution in JT gravity which is characterised by a constant gap (see figure 4b). As the temperature is further increased beyond the critical value $T = T_0$, the charge density starts increasing (see figure 3b). This clearly indicates a transition from Majorana to a hot (complex) SYK phase at finite density. In the dual description, this is what we identify as the charged black hole solution (4.22) in the JT gravity.

6 Concluding remarks

We conclude our analysis by drawing a qualitative comparison with the previous literature [6]. We also add remarks on future directions and the possible generalisations of the present analysis.

6.1 A comparison with [6]

In [6], the authors consider a two-site coupled complex SYK model at finite charge density and investigate its thermal properties using Schwinger-Dyson (SD) equation. For sufficiently low temperatures and weak coupling, they observe a constant gap phase in the spectrum which indicates the possible existence of a wormhole phase. Furthermore, at high temperatures, the phase diagram of this configuration is conjectured to be the holographic dual of a two black hole system.

The authors further notice that for sufficiently small range of parameters (chemical potential and coupling constant)¹² there exists an “intermediate” charged wormhole phase

¹²Notice that, the chemical potential and the coupling constant are two independent parameters of their analysis.

that glues together the “cold” wormhole phase and the two black hole phase at high temperatures.

However, on the other hand, in our analysis the intermediate phase appears to be a Majorana SYK rather than the complex SYK [6]. Despite of these differences, both the previous [6] as well as the present analysis confirm the wormhole to black hole transition using two seemingly different approaches - one is based on the Schwinger-Dyson (SD) equation [6] while the present analysis is based on a gravity calculation in 2D.

6.2 Work in progress and future directions

Recall that, in Section 3 we compute the “annealed” free energy [4] of the wormhole solution and explore the associated phase stability (see Section 5). However, one can further refine the computation by including the corrections due to replica wormholes [28, 29] and compute the “quenched” free energy [4]. Our next goal would be to explore the properties of “quenched” free energy and study the corresponding phase stability of the configuration at finite chemical potential [30].

Below, we list some further generalisations of the present work.

- It would be interesting to generalise the present calculation in the presence of $SU(2)$ Yang-Mills fields and study the phase stability of the configuration. However, it has been found in [27] that $SU(2)$ Yang-Mills fields are responsible for the Hawking-Page transition in 2D gravity. Therefore, we expect a much richer phase structure in this model.

- Finally, one can further generalise the present model in the presence of the higher derivative interactions [26] and look their imprints on the corresponding phase stability.

Acknowledgments

The authors are indebted to the authorities of Indian Institute of Technology, Roorkee for their unconditional support towards researches in basic sciences. DR would like to acknowledge The Royal Society, UK for financial assistance. DR would also like to acknowledge the Grant (No. SRG/2020/000088) received from The Science and Engineering Research Board (SERB), India.

A Green's function

Below, we provide the detailed expressions of Green's functions corresponding to (3.29)

$$\begin{aligned}
G_+(\rho, \theta; \rho', \theta', m) = & - \left(\exp \left[2i\pi m(\theta - \theta')/b + \rho' p_0 + (-2p_0 + \pi p_1)^2/(8p_1) + \{4\rho'(-\pi + \rho')p_1 \right. \right. \\
& + (2q_0 + (\pi + 2\rho')q_1)^2/q_1 \} / 8 \left. \left. \right] \sqrt{\frac{\pi}{2}} \left(\text{Erf} \left[\frac{p_0}{\sqrt{2p_1}} \right] + \text{Erf} \left[\frac{-2p_0 + (\pi - 2\rho')p_1}{2\sqrt{2p_1}} \right] \right) \left(- \text{Erf} \left[\frac{q_0}{\sqrt{2q_1}} \right] \right. \right. \\
& \left. \left. + \text{Erf} \left[\frac{2q_0 + (\pi + 2\rho')q_1}{2\sqrt{2q_1}} \right] \right) \right) / \left(b \left(\exp \left[(2q_0 + (\pi + 2\rho')q_1)^2/8q_1 \right] \left(\text{Erf} \left[\frac{q_0}{\sqrt{2q_1}} \right] - \right. \right. \right. \right. \\
& \left. \left. \left. \text{Erf} \left[\frac{2q_0 + (\pi + 2\rho')q_1}{2\sqrt{2q_1}} \right] \right) \sqrt{p_1} - \exp \left[(-2p_0 + (\pi - 2\rho')p_1)^2/8p_1 \right] \left(\text{Erf} \left[\frac{p_0}{\sqrt{2p_1}} \right] + \right. \right. \right. \\
& \left. \left. \left. \text{Erf} \left[\frac{-2p_0 + (\pi - 2\rho')p_1}{2\sqrt{2p_1}} \right] \right) \sqrt{q_1} \right) \right), \tag{A.1}
\end{aligned}$$

and

$$\begin{aligned}
G_-(\rho, \theta; \rho', \theta', m) = & \left(\exp \left[2i\pi m(\theta - \theta')/b + (2q_0 + \pi q_1)^2/(8q_1) + \{-4(\pi - 2\rho')p_0 + 4p_0^2/p_1 \right. \right. \\
& + (\pi - 2\rho')^2 p_1 + 8\rho' q_0 + 4\rho'(\pi + \rho')q_1 \} / 8 \left. \left. \right] \sqrt{\frac{\pi}{2}} \left(\text{Erf} \left[\frac{p_0}{\sqrt{2p_1}} \right] + \text{Erf} \left[\frac{-2p_0 + (\pi - 2\rho')p_1}{2\sqrt{2p_1}} \right] \right) \right. \\
& \left. \left(- \text{Erf} \left[\frac{q_0}{\sqrt{2q_1}} \right] + \text{Erf} \left[\frac{2q_0 + (\pi + 2\rho')q_1}{2\sqrt{2q_1}} \right] \right) \right) / \left(b \left(\exp \left[(2q_0 + (\pi + 2\rho')q_1)^2/8q_1 \right] \cdot \right. \right. \\
& \left. \left(- \text{Erf} \left[\frac{q_0}{\sqrt{2q_1}} \right] + \text{Erf} \left[\frac{2q_0 + (\pi + 2\rho')q_1}{2\sqrt{2q_1}} \right] \right) \sqrt{p_1} + \exp \left[(-2p_0 + (\pi - 2\rho')p_1)^2/8p_1 \right] \cdot \right. \\
& \left. \left. \left(\text{Erf} \left[\frac{p_0}{\sqrt{2p_1}} \right] + \text{Erf} \left[\frac{-2p_0 + (\pi - 2\rho')p_1}{2\sqrt{2p_1}} \right] \right) \sqrt{q_1} \right) \right). \tag{A.2}
\end{aligned}$$

B Derivation of the anomalous stress tensor

In this Appendix, we present a derivation of the quantum anomalous stress tensor for gauge fields [25]. In particular, we study how the stress tensor transforms under the Weyl transformation

$$g_{\mu\nu}(x) \rightarrow \tilde{g}_{\mu\nu}(x) = e^{2\sigma(x)} g_{\mu\nu}(x). \tag{B.1}$$

The vacuum expectation value of the stress tensor is defined as

$$\langle T^{\mu\nu}(x) \rangle = \frac{1}{\sqrt{-\tilde{g}}} \frac{\delta}{\delta \tilde{g}_{\mu\nu}(x)} S(\tilde{g}_{\alpha\beta}). \tag{B.2}$$

The variation with respect to $\sigma(x)$ can be decomposed as

$$\frac{\delta}{\delta \sigma(x')} = 2\tilde{g}_{\mu\nu}(x') \frac{\delta}{\delta \tilde{g}_{\mu\nu}(x')}. \tag{B.3}$$

Now, we take the variation of (B.2) with respect to the $\sigma(x')$ (B.3), which yields

$$\frac{\delta}{\delta\sigma(x')}(\sqrt{-\tilde{g}} \langle T_\nu^\mu(x) \rangle) = 2\tilde{g}_{\alpha\beta}(x') \frac{\delta}{\delta\tilde{g}_{\alpha\beta}(x')} \left(\tilde{g}_{\gamma\nu}(x) \frac{\delta}{\delta\tilde{g}_{\mu\gamma}(x)} S(\tilde{g}_{\eta\lambda}) \right). \quad (\text{B.4})$$

Using the commutative property, we can rewrite the right hand side of (B.4) as

$$\tilde{g}_{\alpha\beta}(x') \frac{\delta}{\delta\tilde{g}_{\alpha\beta}(x')} \left(\tilde{g}_{\gamma\nu}(x) \frac{\delta}{\delta\tilde{g}_{\mu\gamma}(x)} S(\tilde{g}_{\eta\lambda}) \right) = \tilde{g}_{\gamma\nu}(x) \frac{\delta}{\delta\tilde{g}_{\mu\gamma}(x)} \left(\tilde{g}_{\alpha\beta}(x') \frac{\delta}{\delta\tilde{g}_{\alpha\beta}(x')} S(\tilde{g}_{\eta\lambda}) \right). \quad (\text{B.5})$$

On plugging (B.5) into (B.4), we finally obtain the variation of the quantum stress tensor with respect to the conformal factor

$$\frac{\delta}{\delta\sigma(x')}(\sqrt{-\tilde{g}(x)} \langle T_\nu^\mu(x) \rangle) = 2\tilde{g}_{\gamma\nu}(x) \frac{\delta}{\delta\tilde{g}_{\mu\gamma}(x)} (\sqrt{-\tilde{g}(x')} \langle T_\alpha^\alpha(x') \rangle). \quad (\text{B.6})$$

References

- [1] S. W. Hawking, “Wormholes in Space-Time,” *Phys. Rev. D* **37**, 904-910 (1988) doi:10.1103/PhysRevD.37.904
- [2] S. W. Hawking and D. N. Page, “The spectrum of wormholes,” *Phys. Rev. D* **42**, 2655-2663 (1990) doi:10.1103/PhysRevD.42.2655
- [3] J. Maldacena and X. L. Qi, “Eternal traversable wormhole,” [arXiv:1804.00491 [hep-th]].
- [4] A. M. García-García and V. Godet, “Euclidean wormhole in the Sachdev-Ye-Kitaev model,” *Phys. Rev. D* **103**, no.4, 046014 (2021) doi:10.1103/PhysRevD.103.046014 [arXiv:2010.11633 [hep-th]].
- [5] A. M. García-García and V. Godet, “Half-wormholes in nearly AdS₂ holography,” [arXiv:2107.07720 [hep-th]].
- [6] A. M. García-García, J. P. Zheng and V. Ziogas, “Phase diagram of a two-site coupled complex SYK model,” *Phys. Rev. D* **103**, no.10, 106023 (2021) doi:10.1103/PhysRevD.103.106023 [arXiv:2008.00039 [hep-th]].
- [7] P. Zhang, “More on Complex Sachdev-Ye-Kitaev Eternal Wormholes,” *JHEP* **03**, 087 (2021) doi:10.1007/JHEP03(2021)087 [arXiv:2011.10360 [hep-th]].
- [8] A. M. García-García, Y. Jia, D. Rosa and J. J. M. Verbaarschot, “Replica Symmetry Breaking and Phase Transitions in a PT Symmetric Sachdev-Ye-Kitaev Model,” [arXiv:2102.06630 [hep-th]].
- [9] S. Sahoo, É. Lantagne-Hurtubise, S. Plugge and M. Franz, “Traversable wormhole and Hawking-Page transition in coupled complex SYK models,” *Phys. Rev. Res.* **2**, no.4, 043049 (2020) doi:10.1103/PhysRevResearch.2.043049 [arXiv:2006.06019 [cond-mat.str-el]].

- [10] A. M. García-García, T. Nosaka, D. Rosa and J. J. M. Verbaarschot, “Quantum chaos transition in a two-site Sachdev-Ye-Kitaev model dual to an eternal traversable wormhole,” *Phys. Rev. D* **100**, no.2, 026002 (2019) doi:10.1103/PhysRevD.100.026002 [arXiv:1901.06031 [hep-th]].
- [11] R. Jackiw, “Lower Dimensional Gravity,” *Nucl. Phys. B* **252**, 343-356 (1985) doi:10.1016/0550-3213(85)90448-1
- [12] C. Teitelboim, “Gravitation and Hamiltonian Structure in Two Space-Time Dimensions,” *Phys. Lett. B* **126**, 41-45 (1983) doi:10.1016/0370-2693(83)90012-6
- [13] A. Almheiri and J. Polchinski, “Models of AdS₂ backreaction and holography,” *JHEP* **11**, 014 (2015) doi:10.1007/JHEP11(2015)014 [arXiv:1402.6334 [hep-th]].
- [14] S. Sachdev and J. Ye, “Gapless spin fluid ground state in a random, quantum Heisenberg magnet,” *Phys. Rev. Lett.* **70**, 3339 (1993) doi:10.1103/PhysRevLett.70.3339 [arXiv:cond-mat/9212030 [cond-mat]].
- [15] A. Kitaev, Hidden correlations in the Hawking radiation and thermal noise, talk given at Joint tuesday/thursday theory seminars, University of California, Santa Barbara, CA, U.S.A., 12 February 2015
- [16] A. Kitaev, A simple model of quantum holography (part 1), talk given at KITP strings seminar and entanglement program, University of California, Santa Barbara, CA, U.S.A., 7 April 2015.
- [17] A. Kitaev, A simple model of quantum holography (part 2), talk given at KITP strings seminar and entanglement program, University of California, Santa Barbara, CA, U.S.A., 27 May 2015.
- [18] J. Maldacena and D. Stanford, “Remarks on the Sachdev-Ye-Kitaev model,” *Phys. Rev. D* **94**, no.10, 106002 (2016) doi:10.1103/PhysRevD.94.106002 [arXiv:1604.07818 [hep-th]].
- [19] J. Polchinski and V. Rosenhaus, “The Spectrum in the Sachdev-Ye-Kitaev Model,” *JHEP* **04**, 001 (2016) doi:10.1007/JHEP04(2016)001 [arXiv:1601.06768 [hep-th]].
- [20] A. Kitaev and S. J. Suh, “The soft mode in the Sachdev-Ye-Kitaev model and its gravity dual,” *JHEP* **05**, 183 (2018) doi:10.1007/JHEP05(2018)183 [arXiv:1711.08467 [hep-th]].
- [21] J. M. Maldacena and L. Maoz, “Wormholes in AdS,” *JHEP* **02**, 053 (2004) doi:10.1088/1126-6708/2004/02/053 [arXiv:hep-th/0401024 [hep-th]].
- [22] M. Cadoni and M. Cavaglia, “Cosmological and wormhole solutions in low-energy effective string theory,” *Phys. Rev. D* **50**, 6435-6443 (1994) doi:10.1103/PhysRevD.50.6435 [arXiv:hep-th/9406053 [hep-th]].
- [23] J. Y. Kim, H. W. Lee and Y. S. Myung, “Classical instanton and wormhole solution of type IIB string theory,” *Phys. Lett. B* **400**, 32-36 (1997) doi:10.1016/S0370-2693(97)00320-1 [arXiv:hep-th/9612249 [hep-th]].

- [24] A. Kundu, “Wormholes & Holography: An Introduction,” [arXiv:2110.14958 [hep-th]].
- [25] L. S. Brown and J. P. Cassidy, “Stress Tensors and their Trace Anomalies in Conformally Flat Space-Times,” *Phys. Rev. D* **16**, 1712 (1977) doi:10.1103/PhysRevD.16.1712.
- [26] H. Rathi and D. Roychowdhury, “Holographic JT gravity with quartic couplings,” *JHEP* **10**, 209 (2021) doi:10.1007/JHEP10(2021)209 [arXiv:2107.11632 [hep-th]].
- [27] A. Lala, H. Rathi and D. Roychowdhury, “Jackiw-Teitelboim gravity and the models of a Hawking-Page transition for 2D black holes,” *Phys. Rev. D* **102**, no.10, 104024 (2020) doi:10.1103/PhysRevD.102.104024 [arXiv:2005.08018 [hep-th]].
- [28] N. Engelhardt, S. Fischetti and A. Maloney, “Free energy from replica wormholes,” *Phys. Rev. D* **103**, no.4, 046021 (2021) doi:10.1103/PhysRevD.103.046021 [arXiv:2007.07444 [hep-th]].
- [29] A. Almheiri, T. Hartman, J. Maldacena, E. Shaghoulian and A. Tajdini, “Replica Wormholes and the Entropy of Hawking Radiation,” *JHEP* **05**, 013 (2020) doi:10.1007/JHEP05(2020)013 [arXiv:1911.12333 [hep-th]].
- [30] H. Rathi and D. Roychowdhury, “in preparation”.